First-principles results for electromagnetic properties of *sd* shell nuclei

Archana Saxena* and Praveen C. Srivastava†
Department of Physics, Indian Institute of Technology Roorkee, Roorkee 247 667, India
(Received 6 April 2017; revised manuscript received 10 July 2017; published 21 August 2017)

In this work we present *ab initio* shell-model calculations for electric quadrupole moments and magnetic dipole moments of *sd* shell nuclei using valence-space Hamiltonians derived with two *ab initio* approaches: the in-medium similarity renormalization group (IM-SRG) and the coupled-cluster effective interaction (CCEI). Results are in reasonable agreement with the available experimental data as well as with the results from the phenomenological USDB effective interaction. This work will add more information to the available *ab initio* results for the spectroscopy of *sd* shell nuclei.

DOI: 10.1103/PhysRevC.96.024316

I. INTRODUCTION

The study of atomic nuclei using first principles is an important topic in nuclear structure physics. The anomalous behavior for nuclei close to the drip lines can now be explained using *ab initio* approaches. The inclusion of three-body forces was found to be crucial for explaining the exact location of the drip line for oxygen and calcium isotopes [1,2]. Although *ab initio* calculations are difficult for heavier nuclei, recently spectroscopy of *sd* shell nuclei using different *ab initio* approaches has been reported in the literature. Using the in-medium similarity renormalization group (IM-SRG) approach, *ab initio* predictions for the ground and excited states of doubly open-shell *sd* nuclei have been reported in Ref. [3]. Also *ab initio* coupled-cluster effective interaction (CCEI) was derived and used to calculate the levels in *p* and *sd* shell nuclei successfully [4–6]. A mass-dependent effective Hamiltonian in a $0\hbar\Omega$ model space for the *sd* shell nuclei, starting from a no-core shell-model Hamiltonian in a $4\hbar\Omega$ model space with the realistic J-matrix Inverse Scattering Potential, fitted to nuclei with masses up to $A = 16$ (JISP16) and chiral next-to-next-to-next-to leading order (N3LO) NN interactions, has been reported in Ref. [7]. The recent experimental results of ^{24}F have been theoretically interpreted with IM-SRG in Ref. [8] and a coupled-cluster interpretation has been presented for recently populated levels in ^{25}F [9]. In all these papers, the focus was on the spectroscopy of *p* and *sd* shell nuclei.

In the present work, our motivation is to test the *ab initio* Hamiltonians derived from the two approaches, IM-SRG and CCEI, by calculating electromagnetic properties of *sd* shell nuclei. The results of this work will add to the earlier studies in Refs. [3–5,7], where only spectroscopic properties (spins, parities, and level energies) of these nuclei were reported. We compare our results to the available experimental data as well as with the calculations using the phenomenological USDB shell-model interaction [10].

The paper is organized as follows. In Sec. II, we present the details about the Hamiltonians from *ab initio* approaches. In Sec. III, we present the theoretical results along with the experimental data wherever these are available. Finally, a summary and conclusions are presented in Sec. IV.

*archanasaxena777@gmail.com
†pcsrifph@iitr.ac.in

II. HAMILTONIAN

In this work, we have performed shell-model calculations for which the valence-space Hamiltonian was derived using two modern *ab initio* approaches: in-medium similarity renormalization group (IM-SRG) [3] and coupled-cluster effective interaction (CCEI) [4]. We have also compared the results with calculations using the phenomenological USDB effective interaction [10]. For the diagonalization of the matrices, we have used the shell-model code NUSHELLX [11].

Using in-medium similarity renormalization group (IM-SRG) [12] based on chiral two- and three-nucleon interactions, Stroberg *et al.* derived mass-dependent Hamiltonians for *sd* shell nuclei [3].

The starting Hamiltonian H is normal-ordered with respect to $|\Phi_0\rangle$

$$H = E_0 + \sum_{ij} f_{ij}\{a_i^\dagger a_j\} + \frac{1}{2!^2}\sum_{ijkl}\Gamma_{ijkl}\{a_i^\dagger a_j^\dagger a_l a_k\} + \frac{1}{3!^2}\sum_{ijklmn} W_{ijklmn}\{a_i^\dagger a_j^\dagger a_k^\dagger a_n a_m a_l\}, \quad (1)$$

where the normal-ordered strings of creation and annihilation operators obey $\langle\Phi_0|\{a_i^\dagger \ldots a_j\}|\Phi_0\rangle = 0$. The normal-ordered zero-, one-, two-, and three-body terms are E_0, f_{ij}, Γ_{ijkl}, and W_{ijklmn}, respectively (see Ref. [13] for further details). Here, a continuous unitary transformation, parametrized by the flow parameter s, is applied to the initial normal-ordered A-body Hamiltonian:

$$H(s) = U^\dagger(s)H(0)U(s) = H^d(s) + H^{od}(s), \quad (2)$$

where $H^d(s)$ is the diagonal part of the Hamiltonian and $H^{od}(s)$ is the off-diagonal part of the Hamiltonian. The evolution of $H(s)$ with s is given by

$$\frac{dH(s)}{ds} = [\eta(s), H(s)], \quad (3)$$

where $\eta(s)$ is the anti-Hermitian generator of unitary transformation

$$\eta(s) = \frac{dU(s)}{ds}U^\dagger(s) = -\eta^\dagger(s). \quad (4)$$

The off-diagonal matrix elements become zero as $s \to \infty$ for an appropriate value of $\eta(s)$. Here, the *sd* valence space is

decoupled from the core and higher shells as $s \to \infty$. Now we use this resulting Hamiltonian in the shell-model calculations with $\hbar\Omega = 24$ MeV. Further details about the parameters are given in Ref. [3].

There is another *ab initio* approach, named the coupled-cluster effective interaction, which we use in this paper for calculating the electromagnetic properties of nuclei in the *sd* shell. The effective interaction developed from this approach has already been successfully used to calculate the spectroscopy for open *sd* shell deformed nuclei [4]. For the effective interaction from this approach, we have also used a Hamiltonian which is A- dependent:

$$\hat{H}_A = \sum_{i<j}\left(\frac{(\mathbf{p}_i - \mathbf{p}_j)^2}{2mA} + \hat{V}_{NN}^{(i,j)}\right) + \sum_{i<j<k}\hat{V}_{3N}^{(i,j,k)}. \quad (5)$$

The NN and NNN parts are taken from a next-to-next-to leading order (N2LO) chiral nucleon-nucleon interaction and a next-to-next-to-next-to leading order (N3LO) chiral three-body interaction, respectively. A cutoff scale $\Lambda = 500$ MeV is used for the NN part and $\Lambda = 400$ MeV for the NNN part. These interactions are constructed using the similarity transformation group method (see Ref. [5] for further details). In this approach, a Hartree-Fock ground state in 13 oscillator major shells with $\hbar\Omega = 20$ MeV is used. The CCEI Hamiltonian for shell-model calculations can then be expanded as

$$H_{\mathrm{CCEI}} = H_0^{A_c} + H_1^{A_c+1} + H_1^{A_c+2} + \cdots. \quad (6)$$

Here $H_0^{A_c}$, $H_0^{A_c+1}$, and $H_0^{A_c+2}$ are called core, one-body, and two-body cluster Hamiltonians, respectively. This expansion is known as the valence cluster expansion. Similar to this Hamiltonian, any operator can be expanded in the valence space for the shell-model calculations.

The two-body term is computed using the Okubo-Lee-Suzuki (OLS) similarity transformation. We get a non-Hermitian effective Hamiltonian in this procedure. The metric operator $S^\dagger S$ is used to make the Hamiltonian Hermitian. The resultant effective Hermitian Hamiltonian used for the shell model is $[S^\dagger S]^{1/2} H_{\mathrm{CCEI}} [S^\dagger S]^{-1/2}$. Here, S is a matrix that diagonalizes H_{CCEI}.

Finally, we have also compared our *ab initio* results with the shell-model calculations using the phenomenological USDB interaction. The USDB interaction is fitted to two-body matrix elements [10], originally derived from a G-matrix approach. This interaction is fitted by varying 56 linear combinations of two-body matrix elements.

The shell-model code NUSHELLX@MSU is a set of wrapper codes written by Brown. It uses a proton-neutron basis. With this code, it is possible to diagonalize J-scheme matrix dimensions up to ~100 million.

III. RESULTS AND DISCUSSION

The magnetic dipole moment is defined as the expectation value of the dipole operator in the state with maximum M projection as

$$\mu = \langle J; M = J | \sum_i g_l(i) l_{z,i} + \sum_i g_s(i) s_{z,i} | J; M = J \rangle. \quad (7)$$

Here, g_l and g_s are the orbital and spin gyromagnetic ratios, respectively. By applying the Wigner-Eckart theorem,

$$\mu = \frac{J}{[J(J+1)(2J+1)]^{1/2}} \times \left\langle J || \sum_i g_l(i)\mathbf{j_i} + [g_s(i) - g_l(i)]\mathbf{s_i} || J \right\rangle. \quad (8)$$

The electric quadrupole moment operator is defined as

$$Q_z = \sum_{i=1}^{A} Q_Z(i) = \sum_{i=1}^{A} e_i\left(3z_i^2 - r_i^2\right). \quad (9)$$

The spectroscopic quadrupole moment (Q_s) is defined as

$$Q_s(J) = \langle J, m = J | Q_2^0 | J, m = J \rangle = \sqrt{\frac{J(2J-1)}{(2J+1)(2J+3)(J+1)}} \langle J || Q || J \rangle. \quad (10)$$

We have used the harmonic-oscillator parameter $\hbar\Omega = 45A^{-1/3} - 25A^{-2/3}$ MeV for all the three calculations. The calculated values of the electromagnetic properties of *sd* shell nuclei with $e_p = 1.5e$, $e_n = 0.5e$, and $g_s^{\mathrm{eff}} = g_s^{\mathrm{free}}$ using the two *ab initio* interactions as well as the phenomenological USDB shell-model interaction in the *sd* model space, along with the experimental data, are shown in the Tables I and II. In Ref. [14], the suitable values of g factors and effective charges for *sd* shell nuclei are given. However, in the present work, we have compared magnetic and quadrupole moments with two *ab initio* effective interactions along with phenomenological USDB effective interaction using free-nucleon g factors and standard values of effective charges in our calculations. The magnetic moments have been taken from Ref. [15] and more recent data were obtained from a compilation maintained by Mertzimekis under the IAEA auspices [16]. Recently, the experimental quadrupole moments for *sd* shell nuclei have been evaluated and the recommended values were presented in Ref. [17] along with shell-model calculations using the USD and SDPF-U interactions. We have used these experimental quadrupole moments in Table II. The values not available in this evaluation are taken from the specified references.

The experimental static and dynamic moments for Ne, Na, Mg, and Al isotopes up to 20 neutrons, at the borders of (or inside) the island of inversion, are reported in Refs. [18–32]. For explaining the intruder configuration of neutron-rich nuclei ($\sim N = 20$), we need the *sd-pf* model space. Using the SDPF-U-MIX effective interaction in Ref. [33], it was shown the island of inversion region emerges around $N = 20$ and $N = 28$ for Ne to Al isotopes. The island of inversion is also known as island of deformation, which is due to nucleon-nucleon correlations. Because of the correlation energy, we get a deformed ground-state band and the spherical mean field breaks. The normal-order filling of orbits in the case of island of inversion candidates (^{30}Na, ^{31}Na, ^{31}Mg, and ^{33}Al) vanishes, where ^{33}Al is found to be at the border of the island of inversion [32]. The IM-SRG and CCEI *ab initio* effective interactions contain excitations of particles within different shells (~13 oscillator major shells), projected to a particular *sd* model space. The static and transitional

TABLE I. Comparison of the experimental magnetic dipole moments (μ_N) with the theoretical values calculated using free g factors for sd shell nuclei. The experimental data are taken from Refs. [15,35].

Nuclei	State	E_x (keV)	μ_{expt}	$\mu_{\text{IM-SRG}}$	μ_{CCEI}	μ_{USDB}
^{17}O	$5/2^+$	0	−1.89379(9)	−1.913	−1.913	−1.913
^{18}O	2^+	1982	−0.57(3)	−1.094	−1.022	−0.799
	4^+	3555	2.5(4)	−2.455	−2.438	−2.172
^{19}O	$5/2^+$	0	1.53195(7)	−1.509	−1.518	−1.531
	$3/2^+$	96	−0.72(9)	−0.885	−0.869	−0.945
^{20}O	2^+	1674	0.70(3)	−0.921	−0.926	−0.716
^{17}F	$5/2^+$	0	+4.7213(3)	+4.793	+4.793	+4.793
^{18}F	3^+	937	+1.77(12)	+1.847	+1.826	+1.872
	5^+	1121	+2.86(3)	+2.880	+2.880	+2.880
^{19}F	$1/2^+$	0	+2.628868(8)	+2.917	+2.932	+2.898
	$5/2^+$	197	3.595(13)	+3.560	+3.611	+3.584
^{20}F	2^+	0	+2.09335(9)	+2.171	+2.183	+2.092
^{21}F	$5/2^+$	0	3.9194(12)	+3.393	+3.345	+3.779
^{22}F	4^+	0	(+)2.6944(4)	+2.535	+2.477	+2.540
^{19}Ne	$1/2^+$	0	−1.8846(8)	−2.060	−2.092	−2.037
	$5/2^+$	238	−0.740(8)	−0.608	−0.669	−0.673
^{20}Ne	2^+	1634	+1.08(8)	+1.036	+1.037	+1.020
	4^+	4247	+1.5(3)	+2.086	+2.095	+2.052
^{21}Ne	$3/2^+$	0	−0.661797(5)	−0.665	−0.586	−0.750
	$5/2^+$	351	0.49(4)	−0.350	−0.365	−0.574
^{22}Ne	2^+	1275	+0.65(2)	+0.616	+0.550	+0.748
	4^+	3357	+2.2(6)	+1.623	+1.332	+2.044
^{23}Ne	$5/2^+$	0	−1.077(4)	−0.854	−0.786	−1.050
^{25}Ne	$1/2^+$	0	−1.0062(5)	−0.657	−0.924	−0.928
^{20}Na	2^+	0	+0.3694(2)	+0.390	+0.330	+0.446
^{21}Na	$3/2^+$	0	+2.83630(10)	+2.445	+2.388	+2.489
	$5/2^+$	332	3.7(3)	+3.194	+3.196	+3.355
^{22}Na	3^+	0	+1.746(3)	+1.798	+1.806	+1.791
	1^+	583	+0.523(11)	+0.506	+0.529	+0.518
^{23}Na	$3/2^+$	0	+2.2176556(6)	+1.972	+1.887	+2.098
^{24}Na	4^+	0	+1.6903(8)	+1.377	+1.285	+1.631
	1^+	472	−1.931(3)	+0.908	−0.881	−1.865
^{25}Na	$5/2^+$	0	+3.683(4)	+2.934	+3.361	+3.367
^{26}Na	3^+	0	+2.851(2)	+2.296	+2.360	+2.632
^{27}Na	$5/2^+$	0	+3.895(5)	+3.230	+3.623	+3.647
^{28}Na	1^+	0	+2.426(5)	+2.146	+1.760	+2.081
^{29}Na	$3/2^+$	0	+2.449(8)	+2.181	+2.198	+2.438
^{30}Na	2^+	0	+2.083(10)	+2.245	+2.883	+2.418
^{31}Na	$3/2^+$	0	+2.305(8)	+2.535	+2.551	+2.614
^{21}Mg	$5/2^+$	0	−0.983(7)	−0.342	−0.351	−0.848
^{23}Mg	$3/2^+$	0	−0.5364(3)	−0.305	−0.218	−0.410
^{24}Mg	2^+	1369	+1.076(26)	+1.050	+1.094	+1.026
	4^+	4123	+1.6(12)	+2.103	+2.169	+2.070
	2^+	4238	+1.2(4)	+1.072	+1.062	+1.037
	4^+	6010	+2.0(16)	+2.095	+2.115	+2.048
^{25}Mg	$5/2^+$	0	−0.85545(8)	−0.617	−0.197	−0.849
^{26}Mg	2^+	1809	+1.0(3)	+1.024	+1.281	+1.739
^{27}Mg	$1/2^+$	0	−0.411(2)	+0.197	−0.256	−0.412
^{29}Mg	$3/2^+$	0	+0.9780(6)	+1.114	+1.470	+1.071
^{31}Mg	$1/2^+$	0	−0.88355(15)	−0.563	+1.406	−0.923
^{23}Al	$5/2^+$	0	+3.889(5)	+3.716	+3.681	+3.866
^{24}Al	1^+	426	2.99(9)	+2.660[a]	+2.071	+2.985
^{25}Al	$5/2^+$	0	3.6455(12)	+3.462	+3.142	+3.655
^{26}Al	5^+	0	+2.804(4)	+2.850	+2.907	+2.839
^{27}Al	$5/2^+$	0	+3.6415069(7)	+2.525	+2.461	+3.455
^{28}Al	3^+	0	3.242(5)	+2.718	+2.378	+3.098

TABLE I. (*Continued.*)

Nuclei	State	E_x (keV)	μ_{expt}	$\mu_{\text{IM-SRG}}$	μ_{CCEI}	μ_{USDB}
	2^+	31	+4.3(4)	+1.044	+0.675	+3.215
^{30}Al	3^+	0	3.010(7)	+2.442	+3.455	+3.039
^{31}Al	$(5/2^+)$	0	+3.830(5)	+3.571	+3.863	+3.761
^{32}Al	1^+	0	1.952(2)	+1.485	+1.811	+1.612
^{33}Al	$(5/2^+)$	0	+4.088(5)	+4.012	+4.268	+4.224
^{27}Si	$5/2^+$	0	(−)0.8554(4)	+0.117	+0.337	−0.678
^{28}Si	2^+	1779	+1.1(2)	+1.040	+1.093	+1.031
^{29}Si	$1/2^+$	0	−0.55529(3)	−0.010	−0.575	−0.503
^{30}Si	2^+	2235	+0.8(2)	+0.839	+1.939	+0.732
^{33}Si	$(3/2^+)$	0	1.21(3)	+1.212	+1.803	+1.206
^{28}P	3^+	0	0.312(3)	+1.648	+1.076	+0.302
^{29}P	$1/2^+$	0	1.2346(3)	+0.558	+1.348	+1.133
^{31}P	$1/2^+$	0	+1.13160(3)	+0.081	+1.694	+1.087
	$3/2^+$	1270	+0.30(8)	+0.318	−0.063	+0.167
	$5/2^+$	2230	+2.8(5)	+1.260	+3.097	+2.218
^{32}P	1^+	0	−0.2524(3)	−0.764	+0.177	−0.021
^{31}S	$1/2^+$	0	0.48793(8)	+0.472	−1.003	−0.441
^{32}S	2^+	2231	+0.9(2)	+1.022	+0.980	+1.010
	4^+	4459	+1.6(6)	+2.046	+1.840	+2.028

[a]Here we have reported the shell-model result of the second 1^+ state, because calculated order of levels are $1^+ - 4^+ - 1^+$, while the experimental g.s. is 4^+.

quadrupole moments of nuclei lying in the island of inversion region show a drastic enhancement of quadrupole collectivity compared to neighboring nuclei. This has been attributed to a combination of a reduction in the $N = 20$ shell gap due to the tensor part of the nucleon-nucleon monopole interaction and enhanced quadrupole correlations induced by neutron excitations across this reduced shell gap. The moments of these isotopes have been very well described using the phenomenological shell-model interactions in an enhanced *sd-pf* model space where such neutron excitations are included, as illustrated, e.g., in Refs. [24,27,32,34]. The spectroscopy of other *sd* shell isotopes, including their moments, has been very well described by shell-model calculations in the *sd* valence space using the phenomenological effective interactions, such as USDB [14]. However, the recent *ab initio* calculations reproduce also very well the spectroscopy of these *sd* shell isotopes, even improving an accurate description of their structure. It will be interesting to see how well they reproduce the ground-state static and dynamic moments.

For the oxygen isotopes, the calculated values of the magnetic moments with IM-SRG and CCEI show similar results. We have reported the magnetic moments for $^{17-20}$O and quadrupole moments for $^{17-19}$O isotopes. For ^{17}O, the calculated magnetic moment and quadrupole moment values using all the interactions are similar, because this is the single-particle moment (similarly for ^{17}F). The calculated magnetic moment of the $4_1{}^+$ state of ^{18}O and of the $5/2^+$ (g.s.) for ^{19}O and $2_1{}^+$ state of ^{20}O are showing negative sign, while the sign has not yet been confirmed experimentally. For ^{19}O, both *ab initio* interactions give the opposite sign of the quadrupole moment with USDB interaction; however, the sign from an experiment is not yet confirmed. The calculated value of magnetic moments for ^{17,18,20}F isotopes (g.s. and some isomers) are close to the experimental data. However, *ab initio* interactions give slightly different values in comparison to the experimental data for ^{19,21}F. In the case of quadrupole moments, experimental sign of $^{17-22}$F isotopes are not yet confirmed. All the interactions give the same sign.

The experimental data for magnetic moments of Ne isotopes are available from ^{19}Ne to ^{25}Ne, while the quadrupole moments are available for ^{21,22,23}Ne. In Ref. [36], shell-model results of magnetic moments are reported with USD and CW interactions for odd $^{23-25}$Ne isotopes. Shape changes are reported to occur from collective to single particles in Ne isotopes when moving from ^{19}Ne to ^{25}Ne. It is shown that the magnetic moment is more sensitive than the quadrupole moment for deciding the structure of the nucleus. Our calculated results using *ab initio* approaches for magnetic moments are showing reasonable agreement with the experimental data except for ^{23,25}Ne isotopes. We have reported the quadrupole moments for $^{20-23}$Ne isotopes. Both *ab initio* results are in good agreement with the experimental data. In the case of ^{20}Ne, the calculated Q_{2^+} with all the three interactions is approximately -0.15 e b, while experimental value is $-0.23(3)$ e b.

In the $^{26-31}$Na chain [23], it is claimed that the experimental results of the magnetic moments for $^{26-29}$Na are well described with *sd* model space using the USD Hamiltonian. The disagreement appears for the ^{30,31}Na magnetic moments. The ^{30,31}Na isotopes are suggested to be members of the island of inversion, as shown by Utsuno *et al.* [37]. We have calculated the magnetic moments for the g.s. for $^{20-31}$Na isotopes. In the case of ^{21,22}Na and ^{24}Na, the magnetic moments are also given for the first excited state. The results obtained from *ab initio* approaches for the g.s. are in reasonable agreement with the experimental values (Fig. 1). In the case of ^{24}Na, for the magnetic moment (for the first excited state), the sign is reverse using IM-SRG while CCEI gives the sign which is in agreement with the experimental data. We

TABLE II. Comparison of the experimental quadrupole moments (eb) with the theoretical values calculated by using $e_p = 1.5\,e$ and $e_n = 0.5\,e$.

Nuclei	State	E_x (keV)	Q_{expt}	Q_{IM-SRG}	Q_{CCEI}	Q_{USDB}	Ref.
^{17}O	$5/2^+$	0	−0.02558(22)	−0.0302	−0.0302	−0.0302	[38]
^{18}O	2^+	1982	−0.036(9)	−0.0153	−0.0172	−0.0294	[39]
^{19}O	$5/2^+$	0	0.00362(13)	+0.0003	+0.0005	−0.0026	[17]
^{17}F	$5/2^+$	0	0.0799(34)	−0.0907	−0.0907	−0.0907	[17]
^{18}F	5^+	1121	0.077(5)	−0.1226	−0.1226	−0.1224	[39]
^{19}F	$5/2^+$	197	0.0942(9)	−0.1048	−0.01056	−0.1045	[40]
^{20}F	2^+	0	0.0547(18)	+0.0677	+0.0729	+0.0679	[17]
^{21}F	$5/2^+$	0	0.0943(33)	−0.1180	−0.1175	−0.1199	[17]
^{22}F	4^+	0	0.003(2)	−0.0167	−0.0249	−0.0078	[39]
^{20}Ne	2^+	1634	−0.23(3)	−0.1573	−0.1578	−0.1576	[39]
^{21}Ne	$3/2^+$	0	+0.10155(75)	+0.1127	+0.1109	+0.1119	[17,38]
^{22}Ne	2^+	1257	−0.19(4)	−0.1561	−0.1536	−0.1532	[39]
^{23}Ne	$5/2^+$	0	+0.1429(43)	+0.1728	+0.1699	+0.1629	[17]
^{20}Na	2^+	0	0.1009(88)	+0.0961	+0.100	+0.0946	[17]
^{21}Na	$3/2^+$	0	0.137(12)	+0.1224	+0.1216	+0.1218	[17]
^{22}Na	3^+	0	+0.167(17)	+0.2496	+0.2405	+0.2506	[17]
^{23}Na	$3/2^+$	0	+0.104(1)	+0.1217	+0.1246	+0.1180	[17,41]
^{25}Na	$5/2^+$	0	0.00146(22)	+0.0214	+0.0674	+0.0025	[17]
^{26}Na	3^+	0	0.00521(20)	−0.0056	+0.0239	−0.0051	[17]
^{27}Na	$5/2^+$	0	0.00708(24)	−0.0120	−0.0035	−0.0127	[17]
^{28}Na	1^+	0	0.0389(11)	+0.0539	+0.0368	+0.0495	[17]
^{29}Na	$3/2^+$	0	+0.0842(25)	+0.0737	+0.1046	+0.0791	[17]
^{30}Na	2^+	0	+0.146(1.6)	−0.1122	−0.1048	−0.1149	[42]
^{31}Na	$3/2^+$	0	+0.105(2.5)	+0.0465	+0.0920	+0.0583	[42]
^{23}Mg	$3/2^+$	0	0.1133(37)	+0.1285	+0.1322	+0.1229	[17]
^{24}Mg	2^+	1369	−0.29(3)	−0.1914	−0.1857	−0.1931	[39]
^{25}Mg	$5/2^+$	0	+0.1994(20)	+0.2235	+0.1809	+0.2243	[43]
^{26}Mg	2^+	1809	−0.21(2)	−0.1747	+0.1155	−0.1439	[39]
^{25}Al	$5/2^+$	0	0.249(18)	+0.1949	+0.1813	+0.2018	[17]
^{26}Al	5^+	0	+0.259(29)	+0.3260	+0.294	+0.3028	[17]
^{27}Al	$5/2^+$	0	+0.1466(10)	+0.1563	+0.091	+0.1803	[17,44]
^{28}Al	3^+	0	0.172(12)	+0.2289	+0.1388	+0.1877	[17]
^{31}Al	$5/2^+$	0	0.1365(23)	+0.1836	+0.1320	+0.1706	[32]
^{32}Al	1^+	0	0.0250(21)	+0.0370	+0.006	+0.0310	[17]
^{33}Al	$5/2^+$	0	0.141(3)	+0.1375	+0.1368	+0.1390	[32]
^{27}Si	$5/2^+$	0	0.063(14)	+0.1291	+0.072	+0.1409	[45]
^{28}Si	2^+	1779	+0.16(3)	+0.2332	+0.196	+0.2087	[39]
^{30}Si	2^+	2235	−0.05(6)	+0.0465	+0.1470	+0.0239	[39]
^{32}S	2^+	1941	−0.15(2)	−0.0140	−0.0801	−0.1283	[39]
^{33}S	$3/2^+$	0	−0.0678(13)	−0.1431	−0.0565	−0.0736	[46]

have calculated the quadrupole moments for $^{20-23}$Na and $^{25-31}$Na. For ^{26}Na, *ab initio* IM-SRG interaction is giving same sign of the quadrupole moment as in the phenomenological effective interaction. Experimentally, the sign has not yet been confirmed. In the case of ^{30}Na, the results obtained from theory are far from the experimental value because ^{30}Na is an element of the island of inversion. To explain the quadrupole moment for ^{30}Na, we need pf model space. Utsuno *et al.* [34], performed theoretical calculations in $sdf_{7/2}p_{3/2}$ model space using SDPF-M interaction [47] for ^{27,29}Na isotopes using the Monte Carlo shell-model approach.

For Mg isotopes, the sd shell-model space is able to explain the experimental data reasonably well up to ^{29}Mg with all the three interactions. However, in the case of ^{27}Mg, IM-SRG interaction gives opposite sign with the experimental data. In the case of ^{23}Mg, for $Q(3/2^+)$, the experimental sign has not yet been confirmed. Recently, the sign of magnetic moment has been measured using laser spectroscopy at CERN-ISOLDE [48]. Shell model calculations predict a positive sign for the quadrupole moment. In the case of ^{27}Mg, the negative magnetic moment for the ground state is dominated by the $\nu s_{1/2}$ configuration. The IM-SRG fails to reproduce the correct sign of its magnetic moment, although it is also predicting $\nu s_{1/2}$ configuration for the ground state. For ^{29}Mg, the g.s. spin is $I = 3/2\,(\nu d_{3/2})$, and all interactions give the correct sign of the magnetic moment. The sd model space is not able to reproduce correctly the measured ground state $1/2^+$ for ^{31}Mg. For this isotope, a strongly prolate deformed ground state is reported

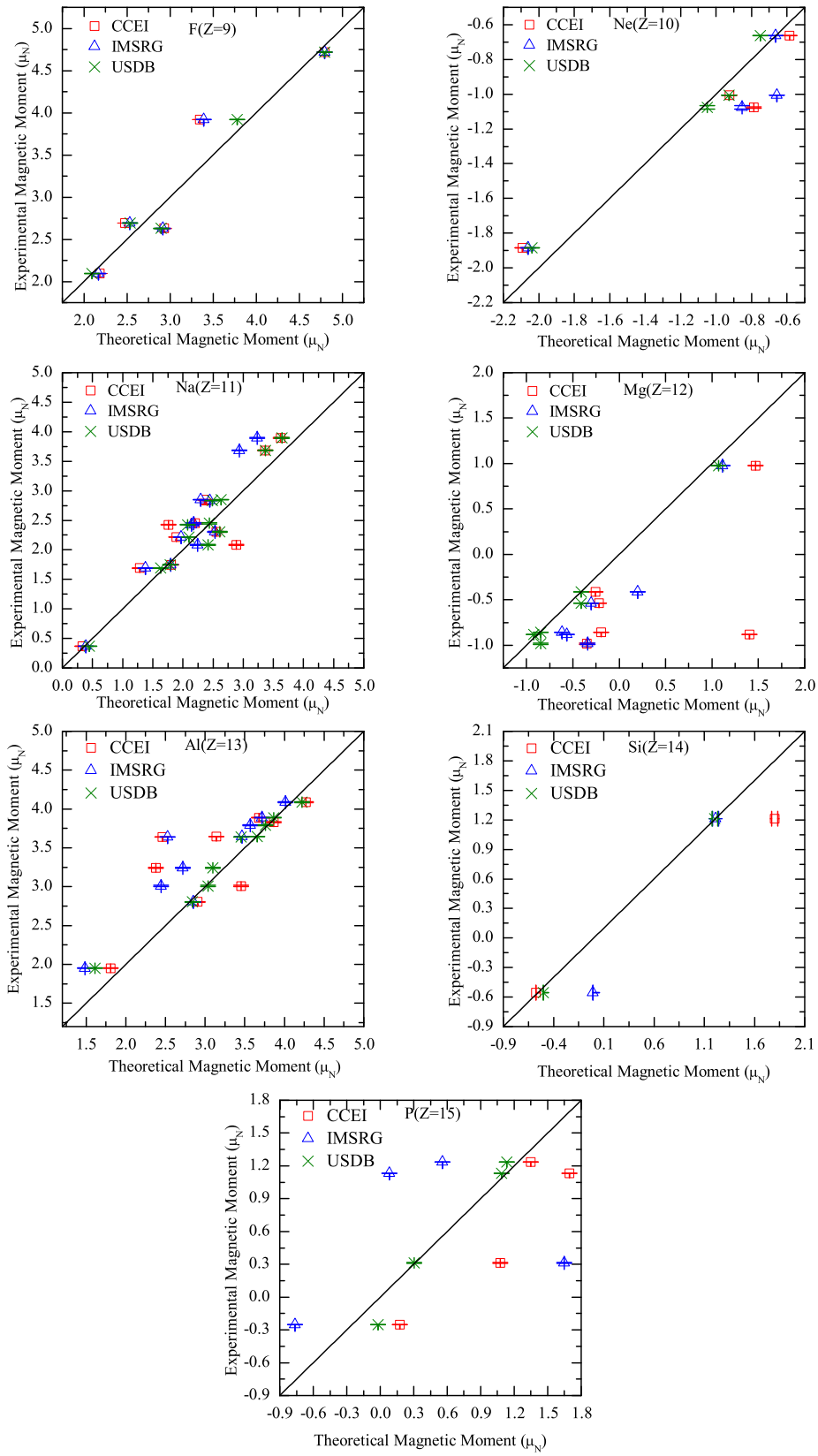

FIG. 1. Comparison between the experimental and theoretical magnetic dipole moments for F, Ne, Na, Mg, Al, Si, and P isotopes. The calculated shell-model signs are used in the cases when it was not measured.

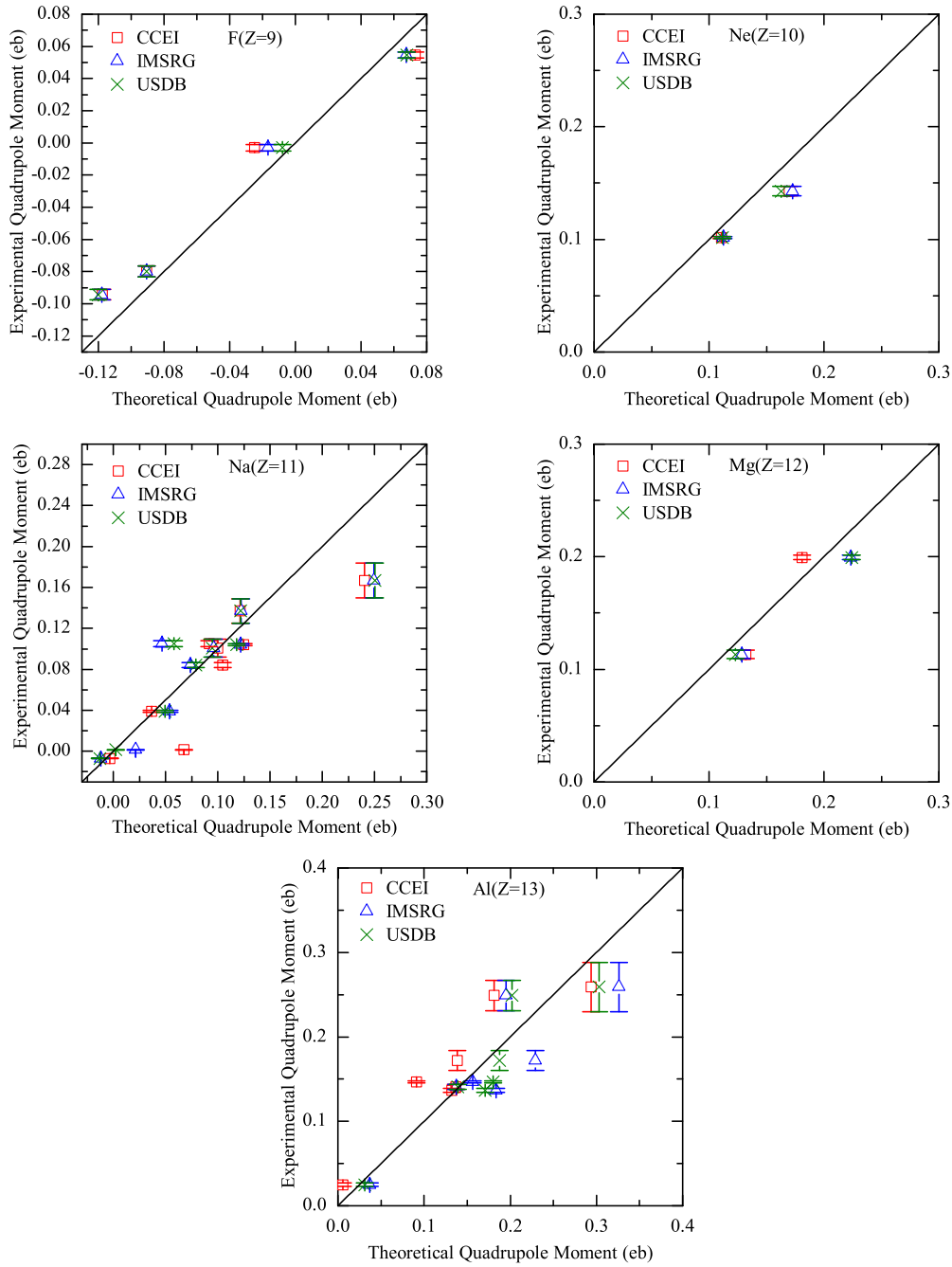

FIG. 2. Comparison between experimental and theoretical quadrupole moments for F, Ne, Na, Mg, and Al isotopes. The calculated shell-model signs are used in case when it was not measured.

in Ref. [20]. Recent theoretical results reveal the existence of 2p-2h and 4p-4h configurations for ^{32}Mg [49].

For $^{25-28,30-33}$Al isotopes, the *sd* model space is able to correctly reproduce the magnetic moments. In most of the isotopes, CCEI results are in reasonable agreement with the experimental data. For ^{25,28,30,32}Al isotopes, the sign for the g.s. magnetic moment is not yet confirmed, theoretically all the three interactions predict positive sign. The calculated $\mu(2^+)$ and $\mu(3^+)$ for ^{28}Al with IM-SRG and CCEI are not showing good agreement with the experimental data. Also, *ab initio* interactions are giving smaller values of the magnetic moment for ^{27}Al. Experimentally, the sign of the quadrupole moment is confirmed only for ^{26,27}Al isotopes. For ^{26}Al, the CCEI result for quadrupole moment is in reasonable agreement with experimental data, while for ^{27}Al, the result of quadrupole moment with IM-SRG is better than CCEI.

In the Si chain, the magnetic moments for ^{27,29,33}Si isotopes are calculated for the g.s. while for ^{28,30}Si isotopes they are for the first excited state. For ^{28,29}Si isotopes, the magnetic moments from the CCEI approach are in reasonable agreement. The calculated $\mu(1/2^+)$ for ^{29}Si is suppressed with IM-SRG in comparison with the experimental data. The *ab initio*

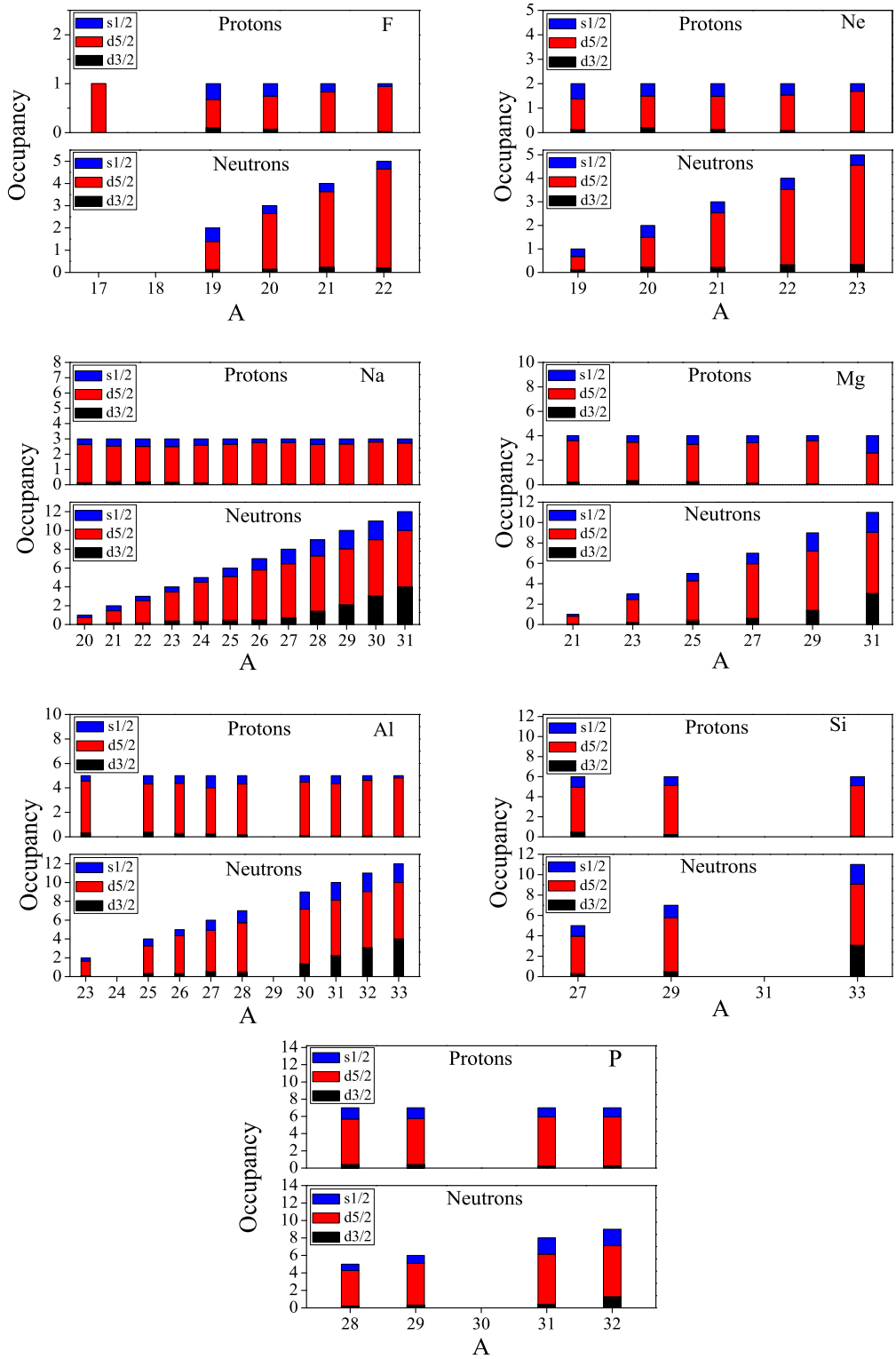

FIG. 3. Occupancies of $d_{3/2}$, $d_{5/2}$, and $s_{1/2}$ proton and neutron orbitals for $^{19-22}$F, $^{19-23}$Ne, $^{20-31}$Na, $^{21-31}$Mg, $^{23,25-28,30-33}$Al, ^{27,29,33}Si, and ^{28,29,31,32}P isotopes with CCEI for the g.s. We have reported occupancies of those nuclei for which the quadrupole and/or magnetic moments are calculated in the present work.

interactions are giving smaller values with the opposite sign of $\mu(5/2^+)$ for ^{27}Si in comparison to the experimental data and with USDB interaction; however, the experimental sign is tentative. The quadrupole moment is calculated for ^{27}Si, ^{28}Si, and ^{30}Si. For ^{30}Si, all the three interactions fail to reproduce the correct sign of the quadrupole moment.

We have also reported the magnetic moments of ^{28,29,31,32}P, and all the calculated results support positive signs for P isotopes in the g.s. except ^{32}P. For ^{32}P, IM-SRG supports the experimental sign but the magnitude is larger in comparison with the experimental value. We have also calculated the magnetic moment of ^{31,32}S and the quadrupole moment of ^{32,33}S. The CCEI results for magnetic moments (^{32}S) and quadrupole moments (^{33}S) are in reasonable agreement with the experimental data.

The calculated g factors with *ab initio* interactions for the yrast levels in even-even $N = Z$ nuclei are $\sim$0.5. Thus, the calculated value is in agreement with the experimental value as reported in Ref. [50].

In Fig. 1, we have shown the comparison between the experimental and theoretical magnetic dipole moments for F, Ne, Na, Mg, Al, Si, and P isotopes. From this figure, it is clear that *ab initio* interactions are not giving values close to the experimental data for heavier Z nuclei. The deviation between the calculated and the experimental data is large for P isotopes. In Figs. 1 and 2, we have shown comparison only for the g.s. of those nuclei which have confirmed experimental signs. Apart from this, we have also plotted the g.s. of those data for which all the interactions are giving the same signs, but their experimental signs are not yet confirmed.

The g.s. quadrupole moments for F, Ne, Na, Mg, and Al isotopes are shown in Fig. 2. All the interactions are giving reasonable results for the F isotopes. For the ^{22}Na, the calculated quadrupole moment is larger in comparison with the experimental data for all the three interactions. For ^{25}Na, *ab initio* interactions give larger $Q(5/2^+)$ values in comparison with the experimental data; however, the result with USDB interaction is reasonable.

The occupancies of $d_{3/2}$, $d_{5/2}$, and $s_{1/2}$ proton and neutron orbitals for $^{19-22}$F, $^{19-23}$Ne, $^{20-31}$Na, $^{21-31}$Mg, $^{23,25-28,30-33}$Al, ^{27,29,33}Si, and ^{28,29,31,32}P isotopes with CCEI for the g.s are shown in Fig. 3. In general, the role of the $d_{5/2}$ orbital is important as neutron number increases.

For ^{30}Na (expt. g.s. is 2^+), IM-SRG and CCEI effective interactions predict g.s. as 0^+, while USDB predicts 2^+. For ^{30}Na, the calculated magnetic moment with IM-SRG interaction is in reasonable agreement with the experimental data; however, all three interactions give opposite signs for quadrupole moment in comparison with the experimental data. For ^{31}Na (experimental g.s. is $3/2^+$), CCEI predicts the correct g.s. while USDB and IM-SRG give $5/2^+$. For this nuclei, the magnetic moments predicted by *ab initio* interactions are similar, whereas the quadrupole moment predicted by CCEI is close to the experimental data. For ^{31}Mg (experimental g.s. is $1/2^+$), *ab initio* and USDB interactions give g.s. of $3/2^+$. The calculated magnetic moment with CCEI is far from the experimental value and also the sign is not correct. For ^{33}Al, all the three interactions give the g.s. as $5/2^+$, although experimentally it is not yet confirmed. The IM-SRG gives value of magnetic moment close to the experimental data for this isotope. In the case of quadrupole moment, sign is not yet confirmed experimentally, but the magnitude is in reasonable agreement with experimental value with all three interactions.

The wave functions of the nuclei which show disagreement between *ab initio* results and with the experimental data and USDB results are shown in Table III. For ^{27}Al, both *ab initio* interactions give same structure. The *ab initio* results for $\mu_{5/2^+}$ are not in a good agreement with the experimental data. In ^{28}Al, the CCEI result for $\mu_{2_1^+}$ is very far from IM-SRG and USDB interactions as well as with the experimental data; also, the wave function is different from IM-SRG and USDB. In the case of CCEI interaction for the ^{28}Al($\mu_{2_1^+}$) result, we have one unpaired proton and one unpaired neutron in $s_{1/2}$ orbits, whereas in USDB and IM-SRG interactions, we have one unpaired neutron in $s_{1/2}$ orbit and one unpaired proton in $d_{5/2}$ orbit. USDB and IM-SRG are also not in very good agreement with the experimental data. In ^{32}Al, all three interactions give the same structure for the wave function but still the CCEI result for $Q_{1_1^+}$ is far from the experimental data. In ^{27}Si, the structure of wave function for CCEI interaction is due to two unpaired protons and one unpaired neutron, whereas in IM-SRG and USDB interactions come from one unpaired neutron in $d_{5/2}$ orbit. In the case of ^{30}Si, the CCEI result for $Q_{2_1^+}$ is very far from the experiment, the structure comes because of the two unpaired protons which are in $s_{1/2}$ and $d_{5/2}$ orbits, while for IM-SRG and USDB interactions two unpaired neutrons are in $d_{3/2}$ and $s_{1/2}$ orbits. For ^{31}P ($\mu_{1/2_1^+}$, $\mu_{5/2_1^+}$), ^{32}S ($Q_{2_1^+}$), and ^{33}S ($Q_{3/2_1^+}$), the structures of wave functions for IM-SRG are very different from USDB and CCEI interactions. For these nuclei, we can see results from Tables I and II that show the IM-SRG results are very far from the experimental data. For ^{28}Na, ^{25}Mg, ^{32}Al, ^{29}Si, and ^{29}P all the three calculations give the same structure of the wave functions. But we can see from Table I a deviation of one of the *ab initio* results with the other two interactions and the experimental data. For ^{28}P, all three calculations give the same structure but the magnitude of USDB result is closer to the experimental data. However, the experimental sign has not yet been confirmed.

IV. SUMMARY

In the present work using two *ab initio* approaches, we have reported the quadrupole and magnetic moments for *sd* shell nuclei with the shell model. We perform calculations with effective interactions derived from in-medium similarity renormalization and coupled-cluster approaches. Along with *ab initio* interactions, we have also compared these results with the phenomenological USDB interaction. The results show reasonable agreement with the available experimental data. This work will add more information to previously known spectroscopic properties of *sd* shell nuclei from *ab initio* approaches.

ACKNOWLEDGMENTS

We would like to thank Gerda Neyens for many useful suggestions and comments on this manuscript. P.C.S. would like to thank S. R. Stroberg for discussions on IM-SRG. A.S. acknowledges financial support from MHRD (Government of India) for her Ph.D. thesis work. P.C.S. acknowledges financial support from faculty initiation grants.

TABLE III. Dominant configuration of the wave functions with *ab initio* effective interactions and USDB effective interaction. In these nuclei, *ab initio* results show deviations with experimental data and USDB effective interaction results.

Nuclei	Spin	IM-SRG	Probability	CCEI	Probability	USDB	Probability
^{28}Na	μ_{1^+}	$\pi\left(d^0_{3/2},d^3_{5/2},s^0_{1/2}\right)\otimes\nu\left(d^1_{3/2},d^6_{5/2},s^2_{1/2}\right)$	41.71%	$\pi\left(d^0_{3/2},d^3_{5/2},s^0_{1/2}\right)\otimes\nu\left(d^1_{3/2},d^6_{5/2},s^2_{1/2}\right)$	43.52%	$\pi\left(d^0_{3/2},d^3_{5/2},s^0_{1/2}\right)\otimes\nu\left(d^1_{3/2},d^6_{5/2},s^2_{1/2}\right)$	51.85%
^{25}Mg	$\mu_{5/2_1{}^+}$	$\pi\left(d^0_{3/2},d^4_{5/2},s^0_{1/2}\right)\otimes\nu\left(d^0_{3/2},d^5_{5/2},s^0_{1/2}\right)$	16.99%	$\pi\left(d^0_{3/2},d^4_{5/2},s^0_{1/2}\right)\otimes\nu\left(d^0_{3/2},d^5_{5/2},s^0_{1/2}\right)$	18.14%	$\pi\left(d^0_{3/2},d^4_{5/2},s^0_{1/2}\right)\otimes\nu\left(d^0_{3/2},d^5_{5/2},s^0_{1/2}\right)$	26.20%
^{27}Al	$\mu_{5/2_1{}^+}$	$\pi\left(d^0_{3/2},d^4_{5/2},s^1_{1/2}\right)\otimes\nu\left(d^0_{3/2},d^5_{5/2},s^1_{1/2}\right)$	6.46%	$\pi\left(d^0_{3/2},d^4_{5/2},s^1_{1/2}\right)\otimes\nu\left(d^0_{3/2},d^5_{5/2},s^1_{1/2}\right)$	12.92%	$\pi\left(d^0_{3/2},d^5_{5/2},s^0_{1/2}\right)\otimes\nu\left(d^0_{3/2},d^6_{5/2},s^0_{1/2}\right)$	27.19%
^{28}Al	$\mu_{3_1{}^+}$	$\pi\left(d^0_{3/2},d^5_{5/2},s^0_{1/2}\right)\otimes\nu\left(d^0_{3/2},d^6_{5/2},s^1_{1/2}\right)$	14.98%	$\pi\left(d^0_{3/2},d^5_{5/2},s^0_{1/2}\right)\otimes\nu\left(d^0_{3/2},d^6_{5/2},s^1_{1/2}\right)$	29.47%	$\pi\left(d^0_{3/2},d^5_{5/2},s^0_{1/2}\right)\otimes\nu\left(d^0_{3/2},d^6_{5/2},s^1_{1/2}\right)$	37.28%
	$\mu_{2_1{}^+}$	$\pi\left(d^0_{3/2},d^5_{5/2},s^0_{1/2}\right)\otimes\nu\left(d^0_{3/2},d^6_{5/2},s^1_{1/2}\right)$	7.72%	$\pi\left(d^0_{3/2},d^4_{5/2},s^1_{1/2}\right)\otimes\nu\left(d^0_{3/2},d^6_{5/2},s^1_{1/2}\right)$	11.66%	$\pi\left(d^0_{3/2},d^5_{5/2},s^0_{1/2}\right)\otimes\nu\left(d^0_{3/2},d^6_{5/2},s^1_{1/2}\right)$	28.15%
^{32}Al	$Q_{1_1{}^+}$	$\pi\left(d^0_{3/2},d^5_{5/2},s^0_{1/2}\right)\otimes\nu\left(d^3_{3/2},d^6_{5/2},s^2_{1/2}\right)$	71.50%	$\pi\left(d^0_{3/2},d^5_{5/2},s^0_{1/2}\right)\otimes\nu\left(d^3_{3/2},d^6_{5/2},s^2_{1/2}\right)$	65.89%	$\pi\left(d^0_{3/2},d^5_{5/2},s^0_{1/2}\right)\otimes\nu\left(d^3_{3/2},d^6_{5/2},s^2_{1/2}\right)$	78.19%
^{27}Si	$\mu_{5/2_1{}^+}$	$\pi\left(d^0_{3/2},d^6_{5/2},s^0_{1/2}\right)\otimes\nu\left(d^0_{3/2},d^5_{5/2},s^0_{1/2}\right)$	9.27%	$\pi\left(d^0_{3/2},d^5_{5/2},s^1_{1/2}\right)\otimes\nu\left(d^0_{3/2},d^4_{5/2},s^1_{1/2}\right)$	13.24%	$\pi\left(d^0_{3/2},d^6_{5/2},s^0_{1/2}\right)\otimes\nu\left(d^0_{3/2},d^5_{5/2},s^0_{1/2}\right)$	27.35%
^{29}Si	$\mu_{1/2_1{}^+}$	$\pi\left(d^0_{3/2},d^6_{5/2},s^0_{1/2}\right)\otimes\nu\left(d^0_{3/2},d^6_{5/2},s^1_{1/2}\right)$	11.62%	$\pi\left(d^0_{3/2},d^6_{5/2},s^0_{1/2}\right)\otimes\nu\left(d^0_{3/2},d^6_{5/2},s^1_{1/2}\right)$	29.18%	$\pi\left(d^0_{3/2},d^6_{5/2},s^0_{1/2}\right)\otimes\nu\left(d^0_{3/2},d^6_{5/2},s^1_{1/2}\right)$	32.52%
^{30}Si	$Q_{2_1{}^+}$	$\pi\left(d^0_{3/2},d^6_{5/2},s^0_{1/2}\right)\otimes\nu\left(d^1_{3/2},d^6_{5/2},s^1_{1/2}\right)$	8.21%	$\pi\left(d^0_{3/2},d^5_{5/2},s^1_{1/2}\right)\otimes\nu\left(d^0_{3/2},d^6_{5/2},s^2_{1/2}\right)$	33.80%	$\pi\left(d^0_{3/2},d^6_{5/2},s^0_{1/2}\right)\otimes\nu\left(d^1_{3/2},d^6_{5/2},s^1_{1/2}\right)$	25.39%
^{28}P	$\mu_{3_1{}^+}$	$\pi\left(d^0_{3/2},d^6_{5/2},s^1_{1/2}\right)\otimes\nu\left(d^0_{3/2},d^5_{5/2},s^0_{1/2}\right)$	8.61%	$\pi\left(d^0_{3/2},d^6_{5/2},s^1_{1/2}\right)\otimes\nu\left(d^0_{3/2},d^5_{5/2},s^0_{1/2}\right)$	29.43%	$\pi\left(d^0_{3/2},d^6_{5/2},s^1_{1/2}\right)\otimes\nu\left(d^0_{3/2},d^5_{5/2},s^0_{1/2}\right)$	37.24%
^{29}P	$\mu_{1/2_1{}^+}$	$\pi\left(d^0_{3/2},d^6_{5/2},s^1_{1/2}\right)\otimes\nu\left(d^0_{3/2},d^6_{5/2},s^0_{1/2}\right)$	10.38%	$\pi\left(d^0_{3/2},d^6_{5/2},s^1_{1/2}\right)\otimes\nu\left(d^0_{3/2},d^6_{5/2},s^0_{1/2}\right)$	28.56%	$\pi\left(d^0_{3/2},d^6_{5/2},s^1_{1/2}\right)\otimes\nu\left(d^0_{3/2},d^6_{5/2},s^0_{1/2}\right)$	32.60%
^{31}P	$\mu_{1/2_1{}^+}$	$\pi\left(d^0_{3/2},d^6_{5/2},s^1_{1/2}\right)\otimes\nu\left(d^2_{3/2},d^6_{5/2},s^0_{1/2}\right)$	6.46%	$\pi\left(d^0_{3/2},d^6_{5/2},s^1_{1/2}\right)\otimes\nu\left(d^0_{3/2},d^6_{5/2},s^2_{1/2}\right)$	66.90%	$\pi\left(d^0_{3/2},d^6_{5/2},s^1_{1/2}\right)\otimes\nu\left(d^0_{3/2},d^6_{5/2},s^2_{1/2}\right)$	34.38%
	$\mu_{3/2_1{}^+}$	$\pi\left(d^0_{3/2},d^6_{5/2},s^1_{1/2}\right)\otimes\nu\left(d^2_{3/2},d^6_{5/2},s^0_{1/2}\right)$	6.44%	$\pi\left(d^0_{3/2},d^6_{5/2},s^1_{1/2}\right)\otimes\nu\left(d^1_{3/2},d^6_{5/2},s^1_{1/2}\right)$	22.13%	$\pi\left(d^1_{3/2},d^6_{5/2},s^0_{1/2}\right)\otimes\nu\left(d^0_{3/2},d^6_{5/2},s^2_{1/2}\right)$	15.28%
	$\mu_{5/2_1{}^+}$	$\pi\left(d^1_{3/2},d^5_{5/2},s^1_{1/2}\right)\otimes\nu\left(d^2_{3/2},d^6_{5/2},s^0_{1/2}\right)$	5.94%	$\pi\left(d^0_{3/2},d^5_{5/2},s^2_{1/2}\right)\otimes\nu\left(d^0_{3/2},d^6_{5/2},s^2_{1/2}\right)$	53.89%	$\pi\left(d^0_{3/2},d^5_{5/2},s^2_{1/2}\right)\otimes\nu\left(d^0_{3/2},d^6_{5/2},s^2_{1/2}\right)$	19.05%
^{32}S	$Q_{2_1{}^+}$	$\pi\left(d^2_{3/2},d^5_{5/2},s^1_{1/2}\right)\otimes\nu\left(d^2_{3/2},d^5_{5/2},s^1_{1/2}\right)$	4.72%	$\pi\left(d^0_{3/2},d^6_{5/2},s^2_{1/2}\right)\otimes\nu\left(d^1_{3/2},d^6_{5/2},s^1_{1/2}\right)$	36.14%	$\pi\left(d^0_{3/2},d^6_{5/2},s^2_{1/2}\right)\otimes\nu\left(d^1_{3/2},d^6_{5/2},s^1_{1/2}\right)$	11.36%
^{33}S	$Q_{3/2_1{}^+}$	$\pi\left(d^2_{3/2},d^6_{5/2},s^0_{1/2}\right)\otimes\nu\left(d^1_{3/2},d^6_{5/2},s^2_{1/2}\right)$	7.93%	$\pi\left(d^0_{3/2},d^6_{5/2},s^2_{1/2}\right)\otimes\nu\left(d^1_{3/2},d^6_{5/2},s^2_{1/2}\right)$	77.18%	$\pi\left(d^0_{3/2},d^6_{5/2},s^2_{1/2}\right)\otimes\nu\left(d^1_{3/2},d^6_{5/2},s^2_{1/2}\right)$	47.69%

[1] T. Otsuka, T. Suzuki, J. D. Holt, A. Schwenk, and Y. Akaishi, Phys. Rev. Lett. **105**, 032501 (2010).
[2] J. D. Holt, T. Otsuka, A. Schwenk, and T. Suzuki, J. Phys. G **39**, 085111 (2012).
[3] S. R. Stroberg, H. Hergert, J. D. Holt, S. K. Bogner, and A. Schwenk, Phys. Rev. C **93**, 051301(R) (2016).
[4] G. R. Jansen, M. D. Schuster, A. Signoracci, G. Hagen, and P. Navrátil, Phys. Rev. C **94**, 011301(R) (2016).
[5] G. R. Jansen, J. Engel, G. Hagen, P. Navratil, and A. Signoracci, Phys. Rev. Lett. **113**, 142502 (2014).
[6] P. C. Srivastava and V. Kumar, Phys. Rev. C **94**, 064306 (2016).
[7] E. Dikmen, A. F. Lisetskiy, B. R. Barrett, P. Maris, A. M. Shirokov, and J. P. Vary, Phys. Rev. C **91**, 064301 (2015).
[8] L. Cáceres, A. Lepailleur, O. Sorlin, M. Stanoiu, D. Sohler, Z. Dombradi, S. K. Bogner, B. A. Brown, H. Hergert, J. D. Holt *et al.*, Phys. Rev. C **92**, 014327 (2015).
[9] Z. Vajta, M. Stanoiu, D. Sohler, G. R. Jansen, F. Azaiez, Z. Dombradi, O. Sorlin, B. A. Brown, M. Belleguic, C. Borcea *et al.*, Phys. Rev. C **89**, 054323 (2014).
[10] B. A. Brown and W. A. Richter, Phys. Rev. C **74**, 034315 (2006).
[11] B. A. Brown and W. D. M. Rae, Nucl. Data Sheets **120**, 115 (2014).
[12] S. K. Bogner, R. J. Furnstahl, and A. Schwenk, Prog. Part. Nucl. Phys. **65**, 94 (2010).
[13] K. Tsukiyama, S. K. Bogner, and A. Schwenk, Phys. Rev. Lett. **106**, 222502 (2011).
[14] W. A. Richter, S. Mkhize, and B. A. Brown, Phys. Rev. C **78**, 064302 (2008).
[15] N. J. Stone, At. Data Nucl. Data Tables **90**, 75 (2005).
[16] IAEA, https://www-nds.iaea.org/nuclearmoments/
[17] M. De Rydt, M. Depuydt, and G. Neyens, At. Data Nucl. Data Tables **99**, 391 (2013).
[18] H. Iwasaki, T. Motobayashi, H. Sakurai, K. Yoneda, T. Gomi, N. Aoi, N. Fukuda, Zs. Fülöp, U. Futakami, Z. Gacsi *et al.*, Phys. Lett. B **620**, 118 (2005).
[19] B. V. Pritychenko, T. Glasmacher, P. D. Cottle, M. Fauerbach, R. W. Ibbotson, K. W. Kemper, V. Maddalena, A. Navin, R. Ronningen, A. Sakharuk *et al.*, Phys. Lett. B **461**, 322 (1999).
[20] G. Neyens, M. Kowalska, D. Yordanov, K. Blaum, P. Himpe, P. Lievens, S. Mallion, R. Neugart, N. Vermeulen, Y. Utsuno, and T. Otsuka, Phys. Rev. Lett. **94**, 022501 (2005).
[21] M. De Rydt, G. Neyens, K. Asahi, D. L. Balabanski, J. M. Daugas, M. Depuydt, L. Gaudefroy, S. Grévy, Y. Hasama, Y. Ichikawa *et al.*, Phys. Lett. B **678**, 344 (2009).
[22] P. Himpe, G. Neyens, D. L. Balabanski, G. Bélier, D. Borremans, J. M. Daugas, F. de Oliveira Santos, M. De Rydt, K. Flanagan, G. Georgiev *et al.*, Phys. Lett. B **643**, 257 (2006).
[23] M. Keim, U. Georg, A. Klein, R. Neugart, M. Neuroth, S. Wilbert, P. Lievens, L. Vermeeren, B. A. Brown (ISOLDE Collaboration), Eur. Phys. J. A **8**, 31 (2000).
[24] P. Doornenbal, H. Scheit, S. Takeuchi, N. Aoi, K. Li, M. Matsushita, D. Steppenbeck, H. Wang, H. Baba, E. Ideguchi *et al.*, Phys. Rev. C **93**, 044306 (2016).
[25] A. M. Hurst, C. Y. Wu, J. A. Becker, M. A. Stoyer, C. J. Pearson, G. Hackman, M. A. Schumaker, C. E. Svensson, R. A. E. Austin, G. C. Ball *et al.*, Phys. Lett. B **674**, 168 (2009).
[26] M. Seidlitz, P. Reiter, R. Altenkirch, B. Bastin, C. Bauer, A. Blazhev, N. Bree, B. Bruyneel, P. A. Butler, J. Cederkall *et al.*, Phys. Rev. C **89**, 024309 (2014).
[27] O. Niedermaier, H. Scheit, V. Bildstein, H. Boie, J. Fitting, R. von Hahn, F. Kock, M. Lauer, U. K. Pal, H. Podlech *et al.*, Phys. Rev. Lett. **94**, 172501 (2005).
[28] M. Seidlitz, D. Mücher, P. Reiter, V. Bildstein, A. Blazhev, N. Bree, B. Bruyneel, J. Cederkäll, E. Clement, T. Davinson *et al.*, Phys. Lett. B **700**, 181 (2011).
[29] J. A. Church, C. M. Campbell, D.-C. Dinca, J. Enders, A. Gade, T. Glasmacher, Z. Hu, R. V. F. Janssens, W. F. Mueller, H. Olliver *et al.*, Phys. Rev. C **72**, 054320 (2005).
[30] D. Borremans, S. Teughels, N. A. Smirnova, D. L. Balabanski, N. Coulier, J.-M. Daugas, F. de Oliveira Santos, G. Georgiev, M. Lewitowicz, I. Matea *et al.*, Phys. Lett. B **537**, 45 (2002).
[31] D. Kameda, H. Ueno, K. Asahi, M. Takemura, A. Yoshimi, T. Haseyama, M. Uchida, K. Shimada, D. Nagae, G. Kijima *et al.*, Phys. Lett. B **647**, 93 (2007).
[32] H. Heylen, M. De Rydt, G. Neyens, M. L. Bissell, L. Caceres, R. Chevrier, J. M. Daugas, Y. Ichikawa, Y. Ishibashi, O. Kamalou *et al.*, Phys. Rev. C **94**, 034312 (2016).
[33] E. Caurier, F. Nowacki, and A. Poves, Phys. Rev. C **90**, 014302 (2014).
[34] Y. Utsuno, T. Otsuka, T. Glasmacher, T. Mizusaki, and M. Honma, Phys. Rev. C **70**, 044307 (2004).
[35] Data extracted using the NNDC World Wide Web site from the ENSDF database.
[36] W. Geithner, B. A. Brown, K. M. Hilligsøe, S. Kappertz, M. Keim, G. Kotrotsios, P. Lievens, K. Marinova, R. Neugart, H. Simon, and S. Wilbert, Phys. Rev. C **71**, 064319 (2005).
[37] Y. Utsuno, T. Otsuka, T. Mizusaki, and M. Honma, Phys. Rev. C **64**, 011301(R) (2001).
[38] D. Sundholm and J. Olsen, J. Phys. Chem. **96**, 627 (1992).
[39] N. J. Stone, At. Data Nucl. Data Tables **111**, 1 (2016).
[40] A. Halkier, O. Christiansen, D. Sundholm, and P. Pyykko, Chem. Phys. Lett. **271**, 273 (1997).
[41] P. Pyykko and A. J. Sadlej, Chem. Phys. Lett. **227**, 221 (1994).
[42] G. Neyens, P. Himpe, D. L. Balabanski, P. Morel, L. Perrot, M. De Rydt, I. Stefan, C. Stodel, J. C. Thomas, N. Vermeulen *et al.*, Eur. Phys. J. Spec. Topics **150**, 149 (2007).
[43] D. Sundholm and J. Olsen, Nucl. Phys. A **534**, 360 (1991).
[44] V. Kellö, A. J. Sadlej, P. Pyykko, D. Sundholm, and M. Tokman, Chem. Phys. Lett. **304**, 414 (1999).
[45] K. Matsuta, T. Minamisono, M. Fukuda, M. Mihara, K. Sato, K. Minamisono, T. Yamaguchi, T. Onishi, T. Miyake, M. Sasaki *et al.*, Nucl. Phys. A **704**, 98c (2002).
[46] D. Sundholm and J. Olsen, Phys. Rev. A **42**, 1160 (1990).
[47] Y. Utsuno, T. Otsuka, T. Mizusaki, and M. Honma, Phys. Rev. C **60**, 054315 (1999).
[48] D. T. Yordanov, M. L. Bissell, K. Blaum, M. De Rydt, C. Geppert, J. Kramer, K. Kreim, M. Kowalska, A. Krieger, P. Lievens *et al.*, J. Phys. G **44**, 075104 (2017).
[49] A. O. Macchiavelli, H. L. Crawford, C. M. Campbell, R. M. Clark, M. Cromaz, P. Fallon, M. D. Jones, I. Y. Lee, M. Salathe, B. A. Brown, and A. Poves, Phys. Rev. C **94**, 051303(R) (2016).
[50] A. Kusoglu, A. E. Stuchbery, G. Georgiev, B. A. Brown, A. Goasduff, L. Atanasova, D. L. Balabanski, M. Bostan, M. Danchev, P. Detistov *et al.*, Phys. Rev. Lett. **114**, 062501 (2015).